environmental sciences
proceedings

MDPI

Proceeding Paper

Investigation of Climate Change Impacts on the Building Materials of Archeological Monuments †

Iason Markantonis [1,2,*], Athanasios Sfetsos [1], Diamando Vlachogiannis [1], Ioannis Kioutsioukis [2], Anastasia Michalopoulou [3], Vassilis Kilikoglou [3] and Ioannis Karatasios [3]

[1] Institute of Nuclear & Radiological Sciences & Technology, Energy & Safety, National Centre for Scientific Research "Demokritos", 15310 Athens, Greece; ts@ipta.demokritos.gr (A.S.); mandy@ipta.demokritos.gr (D.V.)
[2] Department of Physics, University of Patras, 26504 Patras, Greece
[3] Institute of Nanoscience and Nanotechnology, National Centre for Scientific Research "Demokritos", 15310 Athens, Greece
* Correspondence: jasonm@ipta.demokritos.gr
† Presented at the 16th International Conference on Meteorology, Climatology and Atmospheric Physics—COMECAP 2023, Athens, Greece, 25–29 September 2023.

Abstract: Weather conditions affect the microclimate of architectural monuments. The alteration of microclimate conditions may create risks for monuments, accelerating their weathering process. For Greece, hosting numerous monuments, the identification of the risks that climate change possess is essential for planning mitigation actions. The main soluble salts that affect archaeological materials are halite and the system of thenardite/mirabilite. The thermodynamics of the salts' equilibrium are affected by atmospheric conditions. We study the climatology of these conditions, adopting modeled data produced by high-resolution simulations. Possible climate change impacts are investigated, aiming at mapping monuments' vulnerability in Greece.

Keywords: cultural heritage; climate change; salt transitions; halite; mirabilite

Citation: Markantonis, I.; Sfetsos, A.; Vlachogiannis, D.; Kioutsioukis, I.; Michalopoulou, A.; Kilikoglou, V.; Karatasios, I. Investigation of Climate Change Impacts on the Building Materials of Archeological Monuments. *Environ. Sci. Proc.* **2023**, *26*, 120. https://doi.org/10.3390/environsciproc2023026120

Academic Editors: Panagiotis Nastos

Published: 29 August 2023

1. Introduction

Greece is a country with numerous important archaeological sites, architectural monuments, and traditional buildings constructed over a period of thousands of years spanning from the Paleolithic Era to the modern day. Due to their significance, the scientific community is actively engaged in understanding the impact of climate conditions occurring over the centuries and those of the imminent climate change on monuments and archaeological sites [1,2]. Weather conditions have an impact on the preservation of monuments since they affect the condition of their building materials and control the initiation of several weathering mechanisms on their surface [3,4]. Most of the archaeological sites in Greece are in coastal regions or at a short distance from the coastline. In these sites, the main weathering mechanisms are initiated by the transportation, deposition, and crystallization of soluble salts caused by marine aerosols [5]. Therefore, an important goal is the study of the crystallization conditions and weathering mechanisms that can lead to the development of mitigation measures for the preservation of archeological buildings, taking into consideration also possible effects of Climate Change. In this work, we study on a daily basis the occurrence of relative humidity (RH) and temperature (T) conditions that affect the crystallization of salt ions, adopting daily gridded modeled climate data produced by dynamically downscaled high-resolution simulations of 5 km [6]. The Weather Research and Forecasting (WRF) regional model driven by the Global Circulation Model EC-EARTH has provided extensively validated data used in the current study, for the historical (1980–2004) and future periods (2025–2049 and 2075–2099), under Representative Concentration Pathways 4.5 and 8.5 [7–9]. This paper focuses on two different salt transition processes (sodium chloride and sodium sulfate) and their occurrence on an annual and seasonal basis. The interpretation of raw data is presented in figures that exhibit the annual number of events. Additional figures that exhibit the seasonal results have been included in the Supplementary section (Figures S1–S34). The first transition process concerns the crystallization of Halite (NaCl), while the second is the crystallization of Thernadite ($Na_2(SO_4)$) and its hydration to Mirabilite ($Na_2SO_4{\cdot}10H_2O$). Moreover, it was examined the annual occurrences of these transitions for the 13 archaeological sites shown and described in Figure 1 the supplementary material. These results have also been included in the Supplementary section.

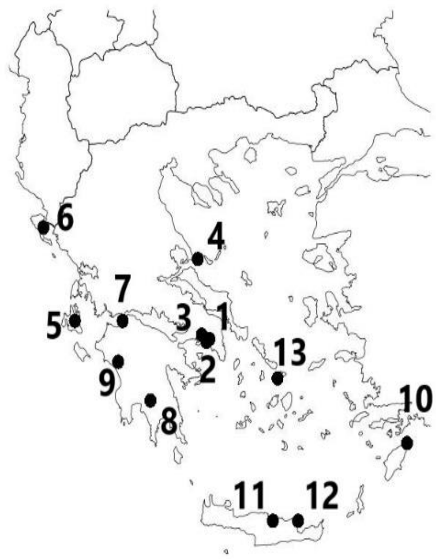

	Monument	*latitude*	*longitude*
1	**Kerameikos**	37.98	23.72
2	**Zea Theater**	37.94	23.64
3	**Elefsis**	38.04	23.54
4	**Panagia Kechria Skiathos**	39.16	23.45
5	**Sami Kefallonia**	38.25	20.64
6	**Old fortress Corfu**	39.62	19.93
7	**Apollon Theater Patras**	38.25	21.74
8	**I.M. Pantanassa Mistras**	37.07	22.37
9	**Ancient Olympia**	37.64	21.63
10	**Medieaval City Rhodes**	36.44	28.22
11	**Knossos**	35.30	25.16
12	**Spinalonga**	35.30	25.74
13	**Delos**	37.40	25.27

Figure 1. Map of the 13 monuments with the name, the latitude, and the longitude.

2. Methodology

RH is the main factor at both salt transitions, while temperature affects only the transition of Thernadite to Mirabilite. The gridded dataset adopted contains 4 values in a span of 24 h, i.e., every 6 h. For our calculations, we have obtained the minimum (RHmin), mean (RHmean), and maximum (RHmax) of RH, and similarly, the minimum (TN), mean (TM), and maximum (TX) of T at 2 m above ground level. For Halite, we sum the number of days that RHmin is lower than 75.3% and RHmax is higher than 75.3% [10]. An increase in that number of days could potentially lead to an increased risk for the porous materials on the surface of the buildings. The transitions of Thernadite to Mirabilite follow a more complicated rule since TX must be lower than 32.38 °C and TN higher than 0 °C, while RH must be between two non-constant thresholds as proven experimentally by Steiger and Asmussen [11]. From the performed analysis, we have extracted the equations describing the upper and lower thresholds by fitting a polynomial regression for the upper threshold and a linear regression for the lower threshold, as described in the following equations:

$$\text{RHup} = -0.0122 \times \text{TM}^2 + 0.1218 \times \text{TM} + 98.2847 \quad (1)$$

$$\text{RHlow} = 0.73 \times \text{TM} + 60.58 \quad (2)$$

RHup in Equation (1) and RHlow in Equation (2) are the upper and lower thresholds for the daily values of RHmax and RHmin, respectively. Figure 2 shows the stability diagram (RH vs. T) for the sodium sulfate system as calculated by adopting Equations (1) and (2). The region between the blue and the red line satisfies the conditions for the crystallization of Mirabilite and, consequently, the potential damage initiation on the building surface of building materials.

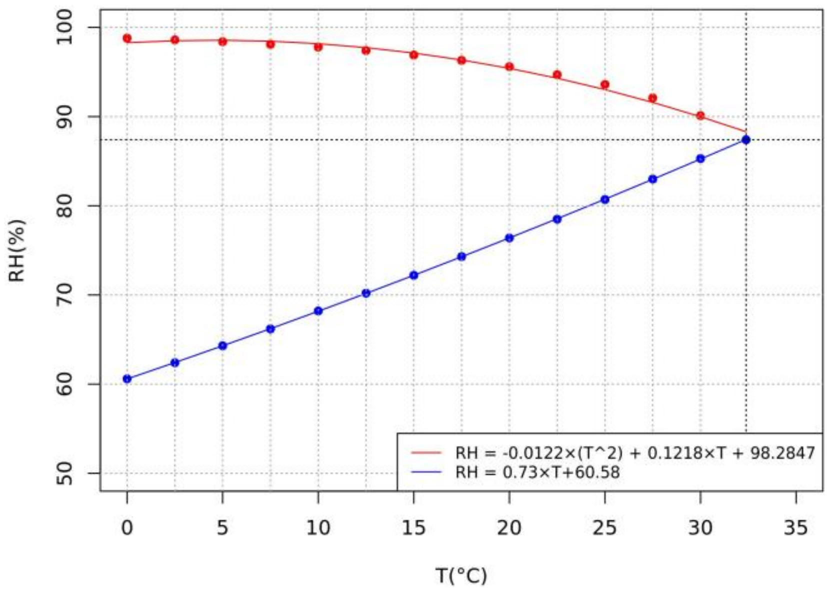

Figure 2. Stability diagram (RH vs. T) for the sodium sulfate system. Equation (1) describes the red line, while Equation (2) describes the blue line. The two lines cross each other at T = 32.38 °C and RH = 87.4% (the point where the dotted lines meet).

3. Results

Each period we examine contains 25 years of daily values; thus, 9132 daily values for the historic period (1980–2004) and 9131 values have been studied for each of the two future periods (2025–2049 and 2075–2099). For our analysis, we have used R coding. In this section, we present the number of events we have computed following the methodology described in the previous section.

3.1. Crystallization of Halite

The past period (Figure 3A) yields the highest values that exceed 200 events per year in the Aegean Islands, the Evros region (Northeast of Greece), and most areas of Western and Northwestern parts of Greece. Most regions yield below 150 events per year. In the future periods (Figure 3B–E), most regions yield a lower number of events than in the past, with the lowest result in RCP8.5 and the 2075–2099 period (Figure 3E). These results imply a lower future damage risk due to halite crystallization. The exception to the above trend is the mountainous areas that yield a higher number of events in all future periods. In Figure S2A, we observe that M/A/M is the season that higher values distributed in lower altitudes and the season that yields the highest positive variances in the future, reaching 17 days in 2075–2099 and RCP8.5 (Figure S1E), mostly in mountainous regions, where we also observe the highest negative variances in values, mainly in Eastern mainland Greece. D/J/F period (Figure S1) exhibits a similar number and distribution of events to M/A/M, while S/O/N (Figure S4) yields the highest values in the Aegean Islands and exhibits positive variance values in RCP8.5 in the 2025–2049 period in Eastern Greece, and negative for the same scenario in most parts of Greece for the 2075–2099 period. The season with the lower number of events is J/J/A (Figure S3A), which exhibits zero or close to zero anomaly values in all future scenarios, apart from RCP8.5 and 2075–2099 (Figure S3E), where we observe the highest negative anomaly values (up to 12 in Northeastern Greece). From the monuments' list under consideration, Delos (Figure S11) is the place with the highest number of events reaching approximately 300 per year while yielding a minor negative trend in the future. The monument that is affected by the fewest number of events is the

Apollon Theater in Patras (Figure S10). The number of events ranges between circa 50 and 110 per year in all periods, with no significant changes between them.

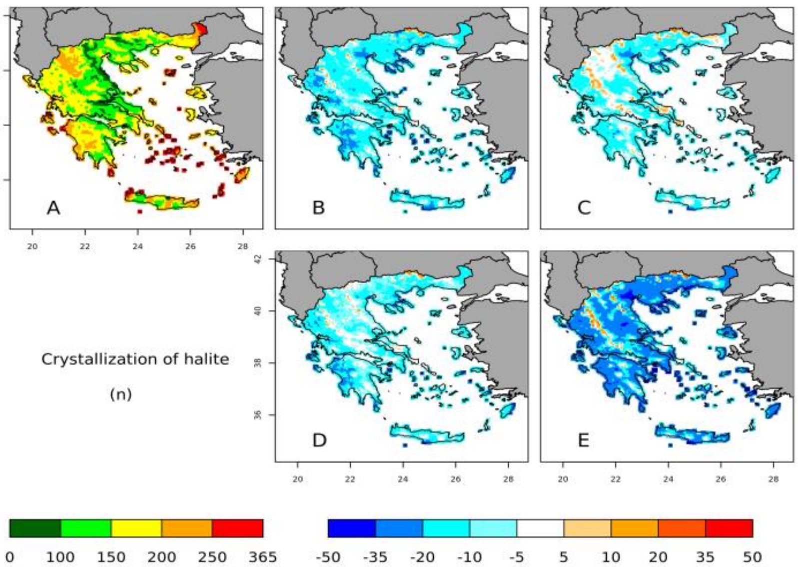

Figure 3. The average number of crystallization events for Halite events per year. (**A**) refers to the 1980–2004 period. (**B**–**E**) show the difference between the historic and the future periods and scenarios. (**B**) depicts the 2025–2049 period and RCP4.5, (**C**) 2075–2099 and RCP4.5, (**D**) the 2025–2049 period and RCP8.5 and (**E**) refers to 2075–2099 period and RCP8.5.

3.2. Crystallization of Thernadite to Mirabilite

Crystallization of Thernadite to Mirabilite yields a lower number of events compared to the crystallization of halite, reaching the highest values (up to 75) in the central Aegean Islands and Northeastern mainland of Greece. Most parts of the country yield negative anomalies in the future, reaching 33 fewer events in the 2075–2099 period and RCP8.5 (Figure 3E), implying a decrease in future risk similar to halite crystallization. The exception to the above trend is the mountainous areas that yield zero or slightly positive anomalies in all scenarios. D/J/F is the season with the highest number of events in most parts of Greece in the past period (Figure S5). The rest of the seasons (Figures S6–S8) yield lower than 10 events per season. Also, D/J/F yields the greatest negative change in values in the coastal regions around Aegean, while on the contrary, the mountainous areas yield the greatest positive anomalies. The rest of the seasons exhibit mostly close to zero negative anomaly values in future scenarios.

All monuments yield lower than 80 events per year in the past period, and the majority show a negative trend in the future. Such an example is Panagia Kechria in Skiathos (Figure S31), where the number of events in the past period range between 30 and 80, while in the future, it ranges between 10 and 60 for the RCP4.5 scenario and between 5 and 50 for RCP8.5. Other monuments, like the Medieval City of Rhodes (Figure S29), are affected by less than 20 events per year, yielding no significant trend in the future for both scenarios.

4. Conclusions

This work attempted to quantify the daily events that satisfy the conditions necessary for the transitions of sodium chloride and sodium sulfate soluble salts. The process for the crystallization of Halite demands simpler criteria to be satisfied than the process for the crystallization of Thernadite and its hydration to Mirabilite. This is justified by the results presented, where a much higher number of events occurred for the first compared to the second process. Both processes yield negative anomaly values in the future period scenarios in most parts of the country. The exception to this is mainly the most mountainous areas of Greece, which yield zero or positive anomaly values. However, the number of events related to these processes does not describe the damage caused but the potential for damage to occur. The results discussed are related to the conditions created on the surface of the building materials, which are affected straightforwardly by the weather conditions. The prediction of possible damage mechanisms below the surface of materials requires a more thorough analysis of additional parameters, such as mineralogy, pore-space characteristics, and mechanical properties of the building materials. Moreover, Greece is covered with monuments constructed across all historic periods, and the exposure of each monument to weather conditions varies in time and intensity, as we observed in Figures 3 and 4. Therefore, future work could focus on monuments located in the areas where the highest number of salt transition events are observed, in order to examine the impacts of the salt transitions in the actual materials of the specific monuments.

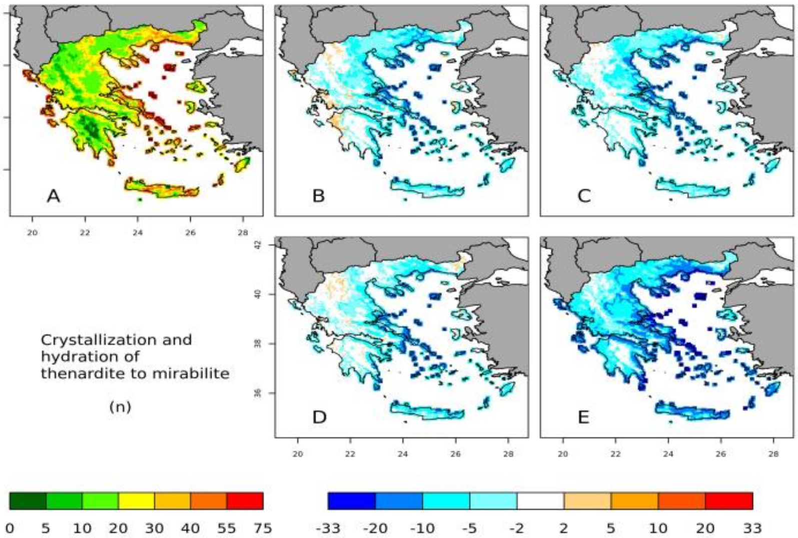

Figure 4. The average number of crystallization of Thernadite to Mirabilite events per year. (**A**) refers to the 1980–2004 period. (**B**–**E**) show the difference between the historic and the future periods and scenarios. (**B**) depicts the 2025–2049 period and RCP4.5, (**C**) the 2075–2099 period and RCP4.5, (**D**) the 2025–2049 period and RCP8.5 and (**E**) refers to the 2075–2099 period and RCP8.5.

Supplementary Materials: The following supporting information can be downloaded at: https://www.mdpi.com/article/10.3390/environsciproc2023026120/s1, Figure S1: Average number of crystallization of halite events per D/J/F season; Figure S2: Average number of crystallization of halite events per M/A/M season; Figure S3: Average number of crystallization of halite events per J/J/A season; Figure S4: Average number of crystallization of halite events per S/O/N season; Figure S5: Average number of crystallization of thernadite to mirabilite events per D/J/F season; Figure S6: Average number of crystallization of thernadite to mirabilite events per M/A/M season; Figure S7: Average number of crystallization of thernadite to mirabilite events per J/J/A season; Figure S8: Average number of crystallization of thernadite to mirabilite events per S/O/N season; Figure S9: Number of crystallization of halite events per year in Ancient Olympia with trend lines with blue for RCP4.5 and with red for RCP8.5 scenarios; Figure S10: Number of crystallization of halite events per year in Apollon Theater of Patras with trend lines with blue for RCP4.5 and with red for RCP8.5 scenarios; Figure S11: Number of crystallization of halite events per year in Delos with trend lines with blue for RCP4.5 and with red for RCP8.5 scenarios; Figure S12: Number of crystallization of halite events per year in Elefsis with trend lines with blue for RCP4.5 and with red for RCP8.5 scenarios; Figure S13: Number of crystallization of halite events per year in I.M. Pantanassa of Mistras with trend lines with blue for RCP4.5 and with red for RCP8.5 scenarios; Figure S14: Number of crystallization of halite events per year in Kerameikos with trend lines with blue for RCP4.5 and with red for RCP8.5 scenarios; Figure S15: Number of crystallization of halite events per year in Knossos with trend lines with blue for RCP4.5 and with red for RCP8.5 scenarios; Figure S16: Number of crystallization of halite events per year in Medieval City of Rhodes with trend lines with blue for RCP4.5 and with red for RCP8.5 scenarios; Figure S17: Number of crystallization of halite events per year in Old fortress of Corfu with trend lines with blue for RCP4.5 and with red for RCP8.5 scenarios; Figure S18: Number of crystallization of halite events per year in Panagia Lechria of Skiathos with trend lines with blue for RCP4.5 and with red for RCP8.5 scenarios; Figure S19: Number of crystallization of halite events per year in Sami Kefallonia with trend lines with blue for RCP4.5 and with red for RCP8.5 scenarios; Figure S20: Number of crystallization of halite events per year in Spinalonga with trend lines with blue for RCP4.5 and with red for RCP8.5 scenarios; Figure S21: Number of crystallization of halite events per year in Zea Theater with trend lines with blue for RCP4.5 and with red for RCP8.5 scenarios; Figure S22: Number of crystallization of thernadite to mirabilite events per year in Ancient Olympia with trend lines with blue for RCP4.5 and with red for RCP8.5 scenarios; Figure S23: Number of crystallization of thernadite to mirabilite events per year in Apollon Theater of Patras with trend lines with blue for RCP4.5 and with red for RCP8.5 scenarios; Figure S24: Number of crystallization of thernadite to mirabilite events per year in Delos with trend lines with blue for RCP4.5 and with red for RCP8.5 scenarios; Figure S25: Number of crystallization of thernadite to mirabilite events per year in Elefsis with trend lines with blue for RCP4.5 and with red for RCP8.5 scenarios; Figure S26: Number of crystallization of thernadite to mirabilite events per year in I.M. Panranassa of Mistras with trend lines with blue for RCP4.5 and with red for RCP8.5 scenarios; Figure S27: Number of crystallization of thernadite to mirabilite events per year in Kerameikos with trend lines with blue for RCP4.5 and with red for RCP8.5 scenarios; Figure S28: Number of crystallization of thernadite to mirabilite events per year in Knossos with trend lines with blue for RCP4.5 and with red for RCP8.5 scenarios; Figure S29: Number of crystallization of thernadite to mirabilite events per year in Medieval city of Rhodes with trend lines with blue for RCP4.5 and with red for RCP8.5 scenarios; Figure S30: Number of crystallization of thernadite to mirabilite events per year in Old fortress of Corfu with trend lines with blue for RCP4.5 and with red for RCP8.5 scenarios; Figure S31: Number of crystallization of thernadite to mirabilite events per year in Pangia Kechria of Skiathos with trend lines with blue for RCP4.5 and with red for RCP8.5 scenarios; Figure S32: Number of crystallization of thernadite to mirabilite events per year in Sami Kefallonia with trend lines with blue for RCP4.5 and with red for RCP8.5 scenarios; Figure S33: Number of crystallization of thernadite to mirabilite events per year in Spinalonga with trend lines with blue for RCP4.5 and with red for RCP8.5 scenarios; Figure S34: Number of crystallization of thernadite to mirabilite events per year in Zea Theater with trend lines with blue for RCP4.5 and with red for RCP8.5 scenarios.

Author Contributions: Conceptualization, I.M., A.S., D.V., I.K. (Ioannis Kioutsioukis) and I.K. (Ioannis Karatasios); methodology, I.M., I.K. (Ioannis Karatasios) and A.M.; software, I.M.; validation, I.M., A.S., D.V. and I.K. (Ioannis Karatasios); formal analysis, I.M.; investigation, I.M., A.M. and I.K. (Ioannis Karatasios); resources, I.K. (Ioannis Karatasios); data curation, I.M.; writing—original draft preparation, I.M.; writing—review and editing, A.S., D.V., I.K. (Ioannis Kioutsioukis) and I.K. (Ioannis Karatasios); visualization, I.M.; supervision, A.S., D.V., I.K. (Ioannis Kioutsioukis) and I.K. (Ioannis Karatasios); project administration, V.K.; funding acquisition, A.S., D.V., V.K. and I.K. (Ioannis Karatasios). All authors have read and agreed to the published version of the manuscript.

Funding: This work was partially supported by the research project "Herisktage–Recording and monitoring systems of the effect of climate change on micro-environment", funded by the Recovery and Resilience Facility-Greek National Recovery and Resilience Plan Greece 2.0, under the action: Protection of Cultural Monuments and Archaeological Sites from Climate Change (Action ID 16433), and financed by the European Union.

Institutional Review Board Statement: Not applicable.

Informed Consent Statement: Not applicable.

Data Availability Statement: All data are available upon request.

Acknowledgments: The authors would like to acknowledge the organizing committee of the 16th International Conference on Meteorology, Climatology and Atmospheric Physics—COMECAP 2023 for the participation in the conference and the special issue published by MDPI.

Conflicts of Interest: The authors declare no conflict of interest.

References

1. Mentzafou, A.; Dimitriou, E. Hydrological Modeling for Flood Adaptation under Climate Change: The Case of the Ancient Messene Archaeological Site in Greece. *Hydrology* **2022**, *9*, 19. [CrossRef]
2. Ravankhah, M.; de Wit, R.; Argyriou, A.V.; Chliaoutakis, A.; Revez, M.J.; Birkmann, J.; Žuvela-Aloise, M.; Sarris, A.; Tzigounaki, A.; Giapitsoglou, K. Integrated Assessment of Natural Hazards, Including Climate Change's Influences, for Cultural Heritage Sites: The Case of the Historic Centre of Rethymno in Greece. *Int. J. Disaster Risk Sci.* **2019**, *10*, 343–361. [CrossRef]
3. Grossi, C.; Brimblecombe, P.; Menéndez, B.; Benavente, D.; Harris, I.; Déqué, M. Climatology of salt transitions and implications for stone weathering. *Sci. Total Environ.* **2011**, *409*, 2577–2585. [CrossRef] [PubMed]
4. Oguchi, C.T.; Yu, S. A review of theoretical salt weathering studies for stone heritage. *Prog. Earth Planet. Sci.* **2021**, *8*, 32. [CrossRef]
5. Michalopoulou, A.; Markantonis, I.; Vlachogiannis, D.; Sfetsos, A.; Kilikoglou, V.; Karatasios, I. Weathering Mechanisms of Porous Marl Stones in Coastal Environments and Evaluation of Conservation Treatments as Potential Adaptation Action for Facing Climate Change Impact. *Buildings* **2023**, *13*, 198. [CrossRef]
6. Politi, N.; Vlachogiannis, D.; Sfetsos, A.; Nastos, P.T. High resolution projections for extreme temperatures and precipitation over Greece. *Clim. Dyn.* **2023**, *61*, 633–667. [CrossRef]
7. Politi, N.; Vlachogiannis, D.; Sfetsos, A.; Nastos, P.T. High-resolution dynamical downscaling of ERA-Interim temperature and precipitation using WRF model for Greece. *Clim. Dyn.* **2021**, *57*, 799–825. [CrossRef]
8. Politi, N.; Sfetsos, A.; Vlachogiannis, D.; Nastos, P.T.; Karozis, S. A Sensitivity Study of High-Resolution Climate Simulations for Greece. *Climate* **2020**, *8*, 44. [CrossRef]
9. Politi, N.; Nastos, P.; Sfetsos, A.; Vlachogiannis, D.; Dalezios, N. Evaluation of the AWR-WRF model configuration at high resolution over the domain of Greece. *Atmos. Res.* **2018**, *208*, 229–245. [CrossRef]
10. Chabas, A.; Jeannette, D.; Lefèvre, R. Crystallization and dissolution of airborne sea-salts on weathered marble in a coastal environment at Delos (Cyclades–Greece). *Atmos. Environ.* **2000**, *34*, 219–224. [CrossRef]
11. Steiger, M.; Asmussen, S. Crystallization of sodium sulfate phases in porous materials: The phase diagram Na_2SO_4–H_2O and the generation of stress. *Geochim. Cosmochim. Acta* **2008**, *72*, 4291–4306. [CrossRef]